
MemControl: Mitigating Memorization in Medical Diffusion Models via Automated Parameter Selection

Raman Dutt¹, Pedro Sanchez¹, Ondrej Bohdal¹, Sotirios A. Tsafaris¹, Timothy Hospedales^{1,2}

¹The University of Edinburgh ²Samsung AI Center, Cambridge
{raman.dutt, pedro.sanchez, ondrej.bohdal, s.tsafaris, t.hospedales}@ed.ac.uk

Abstract

Diffusion models show remarkable ability in generating images that closely mirror the training distribution. However, these models are prone to training data memorization, leading to significant privacy, ethical, and legal concerns, particularly in sensitive fields such as medical imaging. We hypothesize that memorization is driven by the overparameterization of deep models, suggesting that regularizing model capacity during fine-tuning could be an effective mitigation strategy. Parameter-efficient fine-tuning (PEFT) methods offer a promising approach to capacity control by selectively updating specific parameters. However, finding the optimal subset of learnable parameters that balances generation quality and memorization remains elusive. To address this challenge, we propose a bi-level optimization framework that guides automated parameter selection by utilizing memorization and generation quality metrics as rewards. Our framework successfully identifies the optimal parameter set to be updated to satisfy the generation-memorization tradeoff. We perform our experiments for the specific task of medical image generation and outperform existing state-of-the-art training-time mitigation strategies by fine-tuning as few as 0.019% of model parameters. Furthermore, we show that the strategies learned through our framework are transferable across different datasets and domains. Our proposed framework is scalable to large datasets and agnostic to the choice of reward functions. Finally, we show that our framework can be combined with existing approaches for further memorization mitigation.

1 Introduction

Diffusion models [1, 2, 3, 4] have demonstrated exceptional proficiency in generating high-quality data across various modalities, including images [5, 6, 7, 8], audio [9, 10] and graphs [11, 12]. They underpin the commercial success of popular products such as *Midjourney*, *Stable Diffusion* and *DALL-E*, which make it possible to generate images based on user queries. The appeal of generative diffusion models lies in their ability to produce high-quality novel images that capture the underlying intricacies of real data. These models have diverse practical applications, for example they can be used for data augmentation that helps train more accurate recognition systems [13]. They can also be helpful for academic research, for example to help with understanding disease progression [14]. One particularly important and potentially transformative use case of synthetic data is for surpassing restrictions on sharing sensitive data.

Generative diffusion models or the generated synthetic data can be shared instead of the original data, addressing privacy concerns while making it possible to drive progress. However, the utility of this approach would be nullified if diffusion models were to *inadvertently* disclose part of the underlying training data by generating images that are their near-replicas. This phenomenon is known as *memorization* and has linked diffusion models with various legal and ethical issues [15]. It has singled them out as potentially the least private form of generative models [16].

Privacy risks related to memorization are especially significant in the context of healthcare applications. The risks include exact replication of images, potentially disclosing information about the patient [17] and making it possible to conduct re-identification attacks [18]. In re-identification attacks, models that can identify whether two images belong to the same patient can allow an attacker with partial information to link a memorized synthetic image to the associated patient. The growing concern has inspired the development of methods to mitigate memorization. These methods include training-time interventions such as de-duplication [19, 20] and noise regularizers [21], as well as inference-time mitigations such as token-rewriting [20, 22]. However, a key limitation of the fast and effective token-rewriting methods is their vulnerability to white-box attacks. An attacker with access to the model can simply disable the token-rewriting during inference to extract private data.

In this paper, we introduce a new training-time intervention aimed at addressing memorization in diffusion models. We hypothesize that the overcapacity of large neural networks facilitates memorization, and thus we explore whether regularizing model capacity can mitigate this issue. In domain-specific diffusion models, such as those used for medical imaging, the typical workflow involves starting with a general-purpose diffusion model and fine-tuning it with task-specific data [23]. We posit that there is a trade-off between the extent of fine-tuning and the potential for the model to memorize in-domain medical images. If no fine-tuning is performed, the pre-trained model may not replicate specific in-domain data but will also struggle to generate high-quality domain-specific images. Conversely, extensive fine-tuning will push the model to generate high-quality in-domain images but also increase memorization risk. We investigate whether it is possible to strike an effective balance, constraining the model enough to produce high-quality generations while minimizing memorization.

To this end, we leverage parameter-efficient fine-tuning (PEFT) [24, 25, 26, 27, 28, 29], a set of methods that selectively update specific subsets of parameters during the fine-tuning process. Each PEFT method’s unique approach to freezing versus updating parameters results in a different balance between generation quality and memorization. Our study aims to identify which PEFT strategies can best manage this trade-off, ensuring effective specialization of pre-trained models with minimal risk of memorization. We introduce a bi-level optimization framework designed to search for the optimal set of parameters to update, striking a balance between high-quality generation and minimal memorization. Our empirical results on the MIMIC medical imaging dataset [30] demonstrate a significantly improved quality-memorization tradeoff compared to recent state-of-the-art memorization mitigation techniques [20, 22]. While our method is fast and robust during inference, it does incur additional computational cost during training. We show the potential to mitigate this cost by transferring high-quality updatable parameter subsets across different learning problems. This suggests our discovered fine-tuning strategy could be applied off-the-shelf in new applications, thus providing a versatile and effective solution for generative tasks in sensitive domains.

The key contributions of our work are summarised as follows: **(1)** Empirically demonstrating that reducing model capacity significantly mitigates memorization; **(2)** Highlighting the delicate balance between memorization and generalization and how it is influenced by model capacity (Sec. 4.2); **(3)** Proposing a bi-level optimization framework that automates parameter (capacity) selection to optimize both generative quality and memorization mitigation (Sec. 4.3); and **(4)** Showcasing that the parameter subsets discovered are transferable across different datasets and domains (Sec. 4.4).

2 Related Work

2.1 Memorization in Diffusion Models

Memorization in deep generative models has been explored in several contexts, including training data extraction [31, 16], content replication [21] and data copying [20]. Memorization occurs also in the medical domain and has been observed for brain MRI and chest X-ray data [32, 33], posing risks for example via patient re-identification [18]. Given the significant risks associated with memorization, several strategies have been proposed to mitigate it. Based on evidence that duplicate samples increase memorization, the most straightforward approach involves de-duplicating the training set [16, 19, 34]. However, such approach has been shown to be insufficient [20]. In text-to-image generative models, text conditioning significantly influences memorization and several mitigation strategies have been proposed based on this observation [20, 22, 35].

Memorization mitigation strategies can be categorized into training-time and inference-time methods. Training-time methods include augmenting text input as shown in [20], and can be implemented for example via (1) using multiple captions per image, (2) adding Gaussian noise to text embeddings, (3) adding random words or numbers to text prompts. Among these, adding random words (*RWA*) is shown to be the most effective. Another method, *threshold mitigation*, is based on differences in model output magnitudes between memorized and non-memorized prompts, enabling fast detection and mitigation during training [22]. [35] have introduced a strategy examining cross-attention score differences, observing higher attention concentration on specific tokens in memorized prompts. Other studies have explored injecting a deliberate memorization signal via a watermark and detecting it in generated images with a trained classifier [36] to prevent unintended data usage during training [37].

2.2 Parameter-Efficient Fine-Tuning

Models trained on vast online datasets [38] typically lack domain-specific synthesis capabilities, for example they may not be able to generate medical chest X-ray data [23, 39]. Consequently, additional fine-tuning following the *pre-train fine-tune* paradigm is necessary. While conventional methods update all parameters via full fine-tuning (FT) [23], recent advancements introduce parameter-efficient alternatives [25, 26, 28, 29], achieving comparable performance without full model updates.

PEFT strategies freeze most pre-trained model parameters and fine-tune either existing parameters (selective PEFT) or introduce and fine-tune new ones (additive PEFT). Selective PEFT methods include attention tuning [40], bias tuning [41], and normalization tuning [42], while additive PEFT methods include LoRA [43], SSF [27], SV-DIFF [28], DiffFit [29] and AdaptFormer [44] among others, catering to various visual tasks. PEFT matches or exceeds conventional full fine-tuning [45], including on medical imaging [46]. For text-to-image generation, strategies such as SV-DIFF [28] and DiffFit [29] have been proposed, and they excel in both in-domain and out-of-domain settings [46]. In addition to performance evaluation, bi-level optimization frameworks based on PEFT have been shown to enhance fairness and reduce bias in discriminative tasks [47].

3 Methodology

3.1 Diffusion Model Background

We now summarize the fundamentals of diffusion models. Diffusion models use a forward and reverse diffusion process. A forward diffusion process involves a fixed Markov chain spanning T steps, where each step introduces a pre-determined amount of Gaussian noise. The noise is iteratively added to a data point x_0 drawn from the real data distribution $q(x_0)$ as described by:

$$q(x_t | x_{t-1}) = \mathcal{N}(x_t; \sqrt{1 - \beta_t}x_{t-1}, \beta_t \mathbf{I}), \quad (1)$$

where β_t represents the scheduled variance at step t . Closed-form expression for this process is:

$$x_t = \sqrt{\bar{\alpha}_t}x_0 + \sqrt{1 - \bar{\alpha}_t}\epsilon, \quad (2)$$

where $\bar{\alpha}_t = \prod_{i=1}^t (1 - \beta_i)$.

In the reverse diffusion process, a Gaussian vector x_T sampled from $\mathcal{N}(0, 1)$ undergoes denoising so that it can be mapped onto an image x_0 that belongs to the distribution $q(x)$. At each denoising step, a trained noise predictor ϵ_θ removes the noise $\epsilon_\theta(x_t)$ added to x_0 . The formulation for estimating x_{t-1} is:

$$x_{t-1} = \sqrt{\bar{\alpha}_{t-1}}\hat{x}_0^t + \sqrt{1 - \bar{\alpha}_{t-1}}\epsilon_\theta(x_t), \quad (3)$$

where

$$\hat{x}_0^t = \frac{x_t - \sqrt{1 - \bar{\alpha}_{t-1}}\epsilon_\theta(x_t)}{\sqrt{\bar{\alpha}_t}}. \quad (4)$$

3.2 Memorization and Image-Quality Metrics

Our goal is to learn the optimal parameter subset for fine-tuning, given a PEFT method to limit the amount of memorization while maintaining generated image quality. There are various metrics used in the community to measure both memorization [16, 21] and generation quality [48]. In this section, we introduce the metrics that we use in this paper.

Memorization: Nearest Neighbour Distance The simplest definition of memorization considers an example \hat{x} drawn from the model to be memorized if there is a training example x such that $l(x, \hat{x}) < \delta$ for some distance metric l and threshold δ . This means a training example has been memorized if the model produces a near-replica as a sample. A natural metric for the overall degree of memorization of a model is the average nearest neighbour distance between each synthetic sample and its closest example in the training set. For samples $\{\hat{x}_i\}$ drawn from the model and a training set $\{x_j\}$, we follow [49] and quantify memorization as the average minimum cosine distance (AMD):

$$d^{amd} = \frac{1}{N} \sum_{i=1}^N \min_j l_{\cos}(x_i, x_j). \quad (5)$$

Memorization: Extraction Attack We also evaluate memorization using an image extraction attack described in [16]. The attack involves two main steps: (1) Generating numerous image samples for a given prompt, and (2) Conducting membership inference to identify memorized images. In [16], membership inference is performed using a heuristic that constructs a graph of similar samples and identifies sufficiently large cliques—sets of samples that are all similar to each other. Samples from these cliques are likely to be memorized examples. Similarity is measured using a modified ℓ_2 distance, defined as the maximum ℓ_2 distance across corresponding tiles of the two compared images. A smaller number of extracted images translates to lesser memorization.

Memorization: Denoising Strength Heuristic A limitation of the two measures above is that they are comparatively inefficient to compute. An efficient proxy for memorization based on the magnitude of the diffusion noise prediction was introduced in [22]. It represents the discrepancy between model predictions conditioned on a prompt embedding e_p and an empty string embedding e_ϕ averaged across multiple time steps. The detection metric can be formulated as follows:

$$d^{mem} = \frac{1}{T} \sum_{t=1}^T \|\epsilon_\theta(x_t, e_p) - \epsilon_\theta(x_t, e_\phi)\|_2, \quad (6)$$

for a noise-predictor model ϵ_θ trained on input samples with Gaussian noise x_t at time-step t , incorporating prompt embedding e_p , empty string embedding e_ϕ , and T time steps. A higher value of d^{mem} indicates more substantial memorization [22].

Quality: Fréchet Inception Distance (FID) FID score assesses the image generation quality by computing a multivariate normal distribution between real and synthetic images estimated from the features of a pre-trained image encoder. We use a DenseNet-121 [50] model that is pre-trained on chest X-rays [51] to compute the features.

Quality: BioViL-T Score: BioViL-T [48] is a state-of-the-art vision-language model specifically trained for analyzing chest X-Rays and radiology reports. The model returns a joint score denoting the clinical correlation between an image and a text caption. A greater similarity score indicates a higher quality of generated images with better textual guidance.

3.3 Parameter-Efficient Fine-Tuning

The key idea of PEFT is to fine-tune a very small subset of model parameters $\phi \subset \theta$, i.e. $|\phi| \ll |\theta|$. In our framework, the selection of which parameters are fine-tuned is represented using a binary mask ω that is applied on the model parameters θ . Each element of ω determines if a specific parameter at a specific location in the model should be frozen or fine-tuned. The parameters of the pre-trained model are initially θ_0 , and after fine-tuning on data \mathcal{D}^{train} they change by $\Delta\phi$ compared to their initial values. The fine-tuning process can then be defined via

$$\Delta\phi^* = \arg \min_{\Delta\phi} \mathcal{L}^{base}(\mathcal{D}^{train}; \theta_0 + \omega \odot \Delta\phi),$$

where \mathcal{L}^{base} is the mean squared error in the context of image generation problems.

We aim to determine the optimal mask ω that results in fine-tuning with minimal memorization and the highest image generation quality.

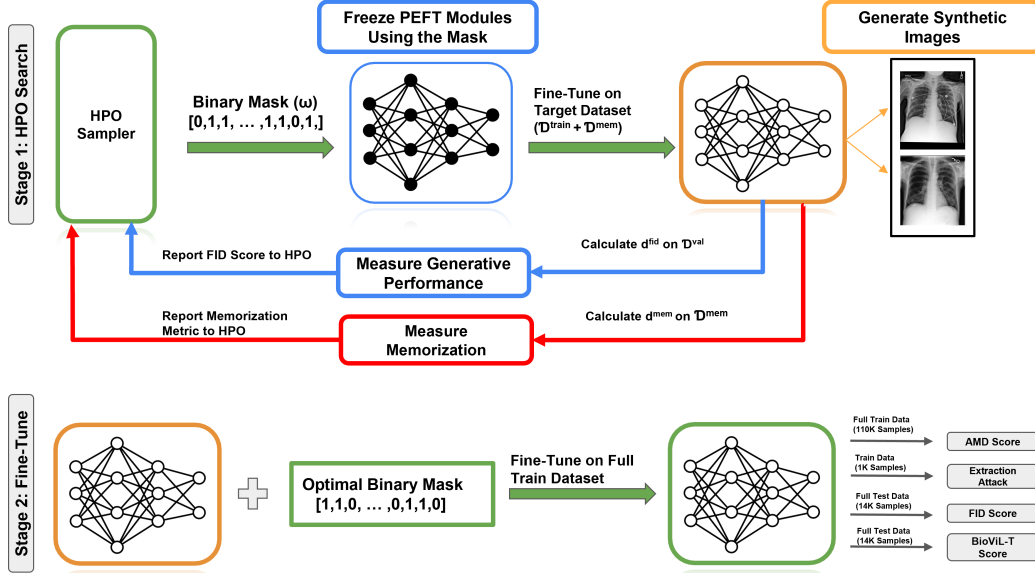


Figure 1: Overall schematic of our framework. **Stage 1: PEFT Mask Search (top):** We use a subset of the training set to search for the mask that decides which PEFT components of a pre-trained model θ should be fine-tuned to optimise both generation quality (d^{fid}) and memorization (d^{mem}). **Stage 2: Fine-tune with mask (bottom):** The optimal mask from the HPO search is used for fine-tuning on full dataset and final results are reported on the test set (\mathcal{D}^{test}).

3.4 Our Method: Optimizing PEFT for Mitigating Memorization

Our method employs a multi-objective bi-level optimization formulation. It trains the model in the inner loop assuming a particular PEFT mask that specifies which diffusion model parameters to freeze or learn. The PEFT mask is optimized in the outer loop so as to obtain a diffusion model with low memorisation and high generation quality. This process is formalized using Eq. 7 and Alg. 1.

$$\omega^* = \underset{\omega}{\operatorname{argmin}} \mathcal{L}^{outer} (d^{mem}(\mathcal{D}^{mem}; \Delta\phi^*), d^{fid}(\mathcal{D}^{val}; \Delta\phi^*)) \quad (7)$$

such that $\Delta\phi^* = \underset{\Delta\phi}{\operatorname{argmin}} \mathcal{L}^{base}(\mathcal{D}^{train}; \theta_0 + \omega \odot \Delta\phi),$

where \mathcal{L}^{base} is the usual diffusion model loss, and $\mathcal{L}^{outer} = (d^{mem}, d^{fid})$ is the two-element vector of memorization and quality objectives respectively (Sec. 3.2). Note that because the outer loop is a multi-objective optimization, ω^* is not a single model, but the set of mask configurations that constitute the pareto front dominating others in terms of memorization and quality. Where necessary, we pick a single model from the pareto front for evaluation by scalarizing the score vector (for example by arithmetic mean) and picking the optimum mask.

The overall workflow first optimizes the mask using a small proxy dataset (see Sec. 4.1) for efficient search, and then fixes a specific optimum mask and re-trains on the full training dataset prior to evaluation (Figure 1).

4 Experiments

4.1 Experimental Setup

Architecture: Our experiments adopted the pre-trained Stable Diffusion (v1.5) [52] model implemented in the *Diffusers* package [53]. The stable diffusion pipeline consists of three components: (1) a modified U-Net [54] with self-attention and cross-attention layers for textual guidance, (2) a text-encoder derived from [55], and a variational auto-encoder [56]. For fine-tuning on medical

Algorithm 1 Optimizing PEFT for Mitigating Memorization

```
1: Input: pre-trained model  $\theta_0$ ,  $\alpha$ : fine-tuning learning rate, number of trials  $T_N$ 
2: Output: fine-tuned model  $\theta_0 + \omega \odot \Delta\phi$  and mask  $\omega$ 
3: while number of completed trials  $< T_N$  do
4:   Initialize  $\Delta\phi = 0$  for  $\phi \leftarrow \phi_0 \subset \theta_0$ 
5:   Propose mask  $\omega \leftarrow HPO$ 
6:   while not converged do
7:      $\Delta\phi \leftarrow \Delta\phi - \alpha \nabla_{\phi} \mathcal{L}^{base}(\mathcal{D}^{train}; \theta_0 + \omega \odot \Delta\phi)$  // PEFT
8:   end while
9:   Evaluate  $d^{mem}$  on  $\mathcal{D}^{mem}$  and  $d^{fid}$  on  $\mathcal{D}^{val}$  with model  $\theta_0 + \omega \odot \Delta\phi$  and report to HPO
10: end while
11: Return the best masks  $\omega$  and fine-tuned models  $\theta_0 + \omega \odot \Delta\phi$ 
```

data we follow previous practice [46, 23], and fine-tune only the U-Net while keeping the other components frozen during our experiments.

Baselines: We compare our approach with different fine-tuning strategies: (1) an off-the-shelf pre-trained Stable Diffusion model that has all of the components frozen, (2) conventional full fine-tuning where every parameter of the U-net is updated, (3) the SV-DIFF PEFT method [28], (4) the DiffFit PEFT method [29], and (4) an Attention tuning PEFT method [40]. Furthermore, we implement existing state-of-the-art training-time memorization-mitigation methods: (1) Random Word Addition (RWA) [20] and threshold mitigation [22]. Overall our main baselines are a combination of four fine-tuning methods and two mitigation strategies.

Search Space and Search Strategy: Our method is based on optimizing the choice of fine-tuning parameters, which requires defining a search space for ω . We conduct our experiments on three different parameter search spaces associated with distinct PEFT methods: **(1) SV-DIFF:** Identifying which attention blocks within the U-Net should include SV-DIFF parameters, **(2) DiffFit:** Identifying which attention blocks within the U-Net should include DiffFit parameters, **(3) Attention Tuning:** Determining which attention layers within the U-Net should be fine-tuned. The search space for both SV-DIFF and DiffFit is $\Omega \in \{0, 1\}^{13}$, while the search space for attention tuning is $\Omega \in \{0, 1\}^{16}$. We also consider an approximate global search over all three search spaces by combining the three pareto fronts from each individual search space. We use the evolutionary search-based NSGA-II Sampler [57] as implemented in *Optuna* [58] to search the space of masks (Eq. 7).

Datasets: We use the MIMIC dataset [30] that consists of chest X-rays and associated radiology text reports. The dataset was split into train, validation and test splits ensuring no leakage of subjects, resulting in 110K training samples, 14K validation and 14K test samples. Note that that several images in this dataset can be associated with the same text prompt due to similarity in clinical findings.

Efficient HPO with a Memorization Subset: Conducting mask search on the whole unaltered training set is infeasible because only a minority of images are memorised, and calculating the memorization metric (Eq. 6, Sec. 3.2) is therefore noisy and slow. To alleviate this, we construct a specific training set \mathcal{D}^{train} for HPO mask search consisting of (1) 1% of the original training set, and (2) a special memorization set \mathcal{D}^{mem} to drive mask search. Specifically, we select 100 text-image pairs from the training set and duplicate them 50 times. With this setup the HPO training set is small, and we know which images are expected to be memorised. HPO mask search is then driven by the two validation objectives d^{mem} and d^{fid} (Eq. 7, Sec. 3.2) which are evaluated on the memorization set \mathcal{D}^{mem} and the validation set \mathcal{D}^{val} respectively. A detailed explanation on memorization subset creation is provided in Appendix C.1.

Experimental Settings: All experiments fine-tune a pre-trained Stable Diffusion model (v1.5) for 20,000 steps with a batch size of 128, using the AdamW optimizer [59]. We employ no warmup steps and utilize a constant learning rate scheduler. Hyperparameter optimization (HPO) search was implemented using *Optuna* package [58]. The final generation quality, indicated by the FID score (d^{fid}) is reported on a held-out test set, and memorization, indicated by the AMD score (d^{amd}), is measured on the training set. The BioViL-T score is measured between the original text captions and generated images from the test set. The extraction attack is conducted between synthetic images and the training set images.

4.2 PEFT Mask Choices Explore the Memorization-Generation Tradeoff

We first explore the influence of model capacity on memorization vs. generalization quality tradeoff by recording the FID score (d^{fid}) and the memorization metric (d^{mem}) for different parameter subsets explored during the HPO search. Each HPO iteration considers a different subset of parameters to freeze or update. The results in Figure 2 show the combined pareto front from searching within the space of SV-Diff [28], DiffFit [29] and Attention Tuning [40] PEFT options. We also report the performance of the defacto full fine-tuning [46, 14], as well as the vanilla configurations of the PEFT methods. From the performance scatter plot, we see that certain configurations favour generation quality ($d^{fid} \downarrow$), others might favour reducing memorization ($d^{mem} \downarrow$) while some can perform poorly on both fronts ($d^{fid} \uparrow, d^{mem} \uparrow$). However, our framework also discovers the Pareto front of configurations that dominate others ($d^{fid} \downarrow, d^{mem} \downarrow$), including configurations that are near optimal for both (bottom left). Importantly, the pareto-front excludes configurations that include the defacto full fine-tuning and PEFT variants.

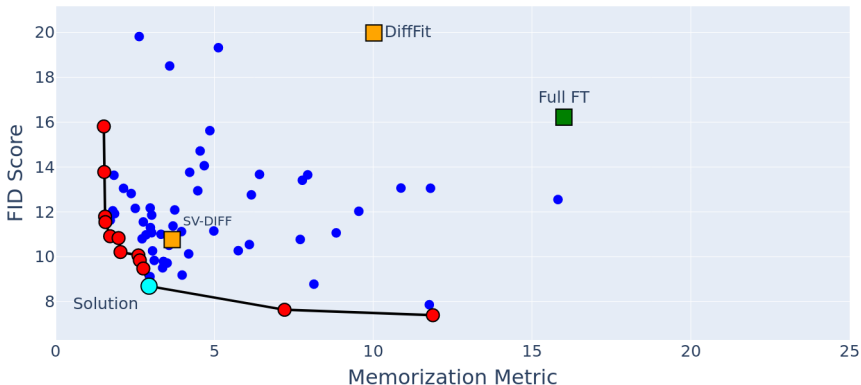


Figure 2: Plot illustrating how model capacity affects the memorization vs. generation quality tradeoff. The Hyperparameter Optimization (HPO) search explored various combinations of parameter subsets during fine-tuning. Each combination results in a different model capacity, generation quality ($d^{fid} \downarrow$) and memorization (d^{mem}, \downarrow). The performance of these subsets is compared to two default PEFT configurations (orange squares) and full fine-tuning (green square). The pareto front of optimal parameter subsets, indicated by the lowest d^{fid} and d^{mem} , are marked in red.

We select a specific model from the Pareto front for further evaluation by taking the mask configuration with the lowest arithmetic mean of FID score ($d^{fid} \downarrow$) and memorisation score ($d^{mem} \downarrow$). Their scale is relatively comparable and both are minimized, so taking their arithmetic mean is reasonable.

4.3 Quantitative Comparison vs. State of the Art

Given the optimal PEFT mask discovered by our framework in Sec. 4.2, we fine-tune using this mask on the full training set, and compare this against competitors. Recall that we consider two types of competitors for memorization mitigation: purpose designed regularisers [20, 22], and alternative PEFT methods [28, 29]. These mitigation methods are independent and potentially complementary, so we also go beyond prior work in reporting all their combinations as well. From the results in Table 1, we observe that: (1) Surprisingly, and despite not being designed to tackle memorization, PEFT methods SV-DIFF [28] and DiffFit [29] outperform state-of-the-art purpose designed mitigation methods such as [22] on several metrics. (2) Our *MemControl* framework achieves the best performance across all metrics. It outperforms both purpose designed mitigation methods, PEFT methods, and their combination across all generation quality and memorization metrics.

Table 1: Comparative evaluation of generation quality (FID ↓, BioViL-T Score ↑) and memorization (AMD ↑, Extracted Images ↓) on the MIMIC dataset. Our MemControl outperforms purpose designed memorization mitigations, standard PEFT methods, and their combinations.

FT Method + Mitigation Strategy	FID Score (↓)	AMD (↑)	BioViL-T Score (↑)	Num. Extracted Images (↓)
Freeze	323.78	0.801	0.23	0
Full FT [23]	35.79	0.029	0.60	356
Full FT [23] + RWA [20]	67.48	0.041	0.58	320
Full FT [23] + Threshold Mitigation [22]	25.43	0.048	0.62	298
SV-DIFF [28]	12.77	0.062	0.72	63
SV-DIFF [28] + RWA [20]	41.25	0.059	0.52	58
SV-DIFF [28] + Threshold Mitigation [22]	23.64	0.068	0.64	45
DiffFit [29]	15.19	0.061	0.69	69
DiffFit [29] + RWA [20]	17.18	0.060	0.67	64
DiffFit [29] + Threshold Mitigation [22]	15.31	0.067	0.69	51
Attn Tuning [40]	40.28	0.031	0.59	358
Attn Tuning [40] + RWA [20]	49.71	0.035	0.52	324
Attn Tuning [40] + Threshold Mitigation [22]	25.43	0.041	0.62	299
MemControl (ours)	11.93	0.114	0.75	28

4.4 PEFT Strategy is Transferable

One might question if a universal approach to balance quality and memorization across multiple datasets exists. To investigate this, we assess the transferability of our PEFT strategy, initially discovered on the MIMIC medical dataset in Sec. 4.2, to a different dataset, namely Imagenette [60], which serves as a smaller and more manageable subset of ImageNet. Specifically, we fine-tune the Stable Diffusion model on Imagenette using the mask derived from MIMIC.

Table 2: Evaluation of generative performance and memorization on Imagenette dataset using parameter subsets learnt from the MIMIC dataset. Our framework leads to the best overall performance in terms of both FID and AMD, showcasing the transferability of strategies from one domain to another.

FT Method + Mitigation Strategy	FID Score (↓)	AMD (↑)
Freeze	62.16	0.101
Full FT	11.01	0.044
Full FT + RWA	8.72	0.048
Full FT + Threshold Mitigation	9.11	0.052
SV-DIFF	8.10	0.058
SV-DIFF + RWA	13.53	0.061
SV-DIFF + Threshold Mitigation	9.38	0.065
DiffFit	7.40	0.054
DiffFit + RWA	11.94	0.058
DiffFit + Threshold Mitigation	12.03	0.062
Attention Tuning	8.04	0.047
Attention Tuning + RWA	9.12	0.049
Attention Tuning + Threshold Mitigation	9.11	0.051
MemControl (ours)	6.34	0.093

The results presented in Table 2 indicate that our *MemControl* method continues to outperform competitors in both generation quality and memorization. This demonstrates the potential for the transferability of fine-tuning masks across datasets, implying that these masks could be reused for new datasets in the future, eliminating the need for repeated mask searches.

4.5 Additional Ablations

MemControl with existing mitigation mechanisms: Our results in Table 3 show that combining *MemControl* with existing mitigation mechanisms leads to improved performance. We do observe a decrease in generation performance in the case of RWA, but its combination with *MemControl* leads to reduced memorization (AMD ↑). A detailed analysis of the performance decrease observed with RWA is provided in Appendix C.2. Combining *MemControl* with Threshold Mitigation leads to the best generation and memorization performance overall.

Table 3: Combining our *MemControl* with existing mitigation strategies (**RWA** [20] and **Threshold Mitigation** [22]) on the MIMIC dataset. Our framework can be seamlessly integrated with these approaches and effectively complement existing methods to enhance memorization mitigation.

Method	FID Score (↓)	AMD (↑)	BioViL-T Score (↑)	Num. Extracted Images (↓)
<i>MemControl</i>	11.93	0.114	0.75	28
<i>MemControl</i> + RWA	13.10	0.121	0.69	23
<i>MemControl</i> + Threshold Mitigation	11.31	0.142	0.75	16

***MemControl* can optimize individual PEFT methods:** Our main result in Table 1 applied *MemControl* across all three PEFT search spaces considered. In Table 4 we demonstrate that when applied to the search space associated with a single PEFT method, *MemControl* can substantially improve its performance.

Table 4: Evaluating *MemControl* in individual parameter search spaces. Our method leads to the best performance in the respective search space defined by distinct PEFT methods (SV-DIFF, DiffFit, Attention Tuning) across all evaluation metrics.

FT Method + Mitigation Strategy	FID Score (↓)	AMD (↑)	BioViL-T (↑)	Num. Extracted Images (↓)
SV-DIFF	12.77	0.062	0.72	63
SV-DIFF + RWA	41.25	0.059	0.52	58
SV-DIFF + Threshold Mitigation	23.64	0.068	0.64	45
<i>MemControl</i> (SV-DIFF Search Space)	11.93	0.114	0.75	28
DiffFit	15.19	0.061	0.69	69
DiffFit + RWA	17.18	0.060	0.67	64
DiffFit + Threshold Mitigation	15.31	0.067	0.69	51
<i>MemControl</i> (DiffFit Search Space)	12.21	0.086	0.72	42
Attn Tuning	40.28	0.031	0.59	358
Attn Tuning + RWA	49.71	0.035	0.52	324
Attn Tuning + Threshold Mitigation	25.43	0.041	0.62	299
<i>MemControl</i> (Attn Tuning Search Space)	22.36	0.044	0.063	281

4.6 Analyzing the Best Solution

Our best solution relied on a subset of SV-DIFF learnable parameters. We analyze the mask indicating which subset of parameters should be fine-tuned. It indicates necessity of fine-tuning all of the cross-attention layers in the Stable Diffusion U-Net, which strongly aligns with the findings in [28]. Additionally, the mask suggests fine-tuning all of the self-attention layers except for those in down-blocks 2 and 3 and up-blocks 3 and 4. Adopting this strategy corresponds to fine-tuning 0.019% of the parameters in Stable Diffusion U-Net.

4.7 Discussion and Limitations

A limitation of our method is its higher computational demand compared to baselines (see Appendix B for details). However, our results indicate that the discovered mask exhibits transferability, implying that repeated mask learning for each new dataset may not be necessary. This means the computational cost of mask search could be incurred once and then amortized over multiple deployments across different datasets. While our approach significantly reduces memorization, it does not completely eliminate it, especially in cases where the PEFT masks are reused across different downstream scenarios. Therefore more work is necessary to completely solve this problem.

5 Conclusion

In this paper, we approached the challenge of mitigating memorization in diffusion models from a parameter-efficient fine-tuning capacity control perspective. We illustrated how the selection of fine-tuning parameter space influences the balance between memorization and generation quality. By searching for PEFT masks, we identified configurations that offer a promising trade-off between generation fidelity and memorization. This introduces a novel and distinctive approach to address the significant memorization issue in diffusion models, contrasting with current mainstream regularization- and token rewriting-based methods.

References

- [1] Jascha Sohl-Dickstein, Eric Weiss, Niru Maheswaranathan, and Surya Ganguli. Deep unsupervised learning using nonequilibrium thermodynamics. In Francis Bach and David Blei, editors, *Proceedings of the 32nd International Conference on Machine Learning*, volume 37 of *Proceedings of Machine Learning Research*, pages 2256–2265, Lille, France, 07–09 Jul 2015. PMLR.
- [2] Jiaming Song, Chenlin Meng, and Stefano Ermon. Denoising diffusion implicit models. In *International Conference on Learning Representations*, 2021.
- [3] Jonathan Ho, Ajay Jain, and Pieter Abbeel. Denoising diffusion probabilistic models. In H. Larochelle, M. Ranzato, R. Hadsell, M.F. Balcan, and H. Lin, editors, *Advances in Neural Information Processing Systems*, volume 33, pages 6840–6851. Curran Associates, Inc., 2020.
- [4] Yang Song, Jascha Sohl-Dickstein, Diederik P Kingma, Abhishek Kumar, Stefano Ermon, and Ben Poole. Score-based generative modeling through stochastic differential equations. In *International Conference on Learning Representations*, 2021.
- [5] Prafulla Dhariwal and Alexander Quinn Nichol. Diffusion models beat GANs on image synthesis. In A. Beygelzimer, Y. Dauphin, P. Liang, and J. Wortman Vaughan, editors, *Advances in Neural Information Processing Systems*, 2021.
- [6] Tero Karras, Samuli Laine, and Timo Aila. A style-based generator architecture for generative adversarial networks. In *Proceedings of the IEEE/CVF conference on computer vision and pattern recognition*, 2019.
- [7] Aditya Ramesh, Prafulla Dhariwal, Alex Nichol, Casey Chu, and Mark Chen. Hierarchical text-conditional image generation with clip latents. *arXiv:2204.06125*, 2022.
- [8] Robin Rombach, Andreas Blattmann, Dominik Lorenz, Patrick Esser, and Björn Ommer. High-resolution image synthesis with latent diffusion models. In *Proceedings of the IEEE/CVF conference on computer vision and pattern recognition*, pages 10684–10695, 2022.
- [9] Heeseung Kim, Sungwon Kim, and Sungroh Yoon. Guided-tts: A diffusion model for text-to-speech via classifier guidance. In *International Conference on Machine Learning*, pages 11119–11133. PMLR, 2022.
- [10] Rongjie Huang, Jiawei Huang, Dongchao Yang, Yi Ren, Luping Liu, Mingze Li, Zhenhui Ye, Jinglin Liu, Xiang Yin, and Zhou Zhao. Make-an-audio: Text-to-audio generation with prompt-enhanced diffusion models. In *International Conference on Machine Learning*, pages 13916–13932. PMLR, 2023.
- [11] Minkai Xu, Lantao Yu, Yang Song, Chence Shi, Stefano Ermon, and Jian Tang. Geodiff: A geometric diffusion model for molecular conformation generation. In *International Conference on Learning Representations*, 2022.
- [12] Clement Vignac, Igor Krawczuk, Antoine Siraudin, Bohan Wang, Volkan Cevher, and Pascal Frossard. Digress: Discrete denoising diffusion for graph generation. In *The Eleventh International Conference on Learning Representations*, 2023.
- [13] Brandon Trabucco, Kyle Doherty, Max A Gurinas, and Ruslan Salakhutdinov. Effective data augmentation with diffusion models. In *The Twelfth International Conference on Learning Representations*, 2024.
- [14] Sourav Kumar, Shell Xu Hu, Timothy Hospedales, Praveer Singh, and Jayashree Kalpathy-cramer. Monitoring disease progression with stable diffusion- a visual approach. In *Medical Imaging with Deep Learning*, 2024.
- [15] Matthew Butterick. Stable diffusion litigation · joseph saveri law firm & matthew butterick, Jan 2023.
- [16] Nicolas Carlini, Jamie Hayes, Milad Nasr, Matthew Jagielski, Vikash Sehwal, Florian Tramèr, Borja Balle, Daphne Ippolito, and Eric Wallace. Extracting training data from diffusion models. In *32nd USENIX Security Symposium (USENIX Security 23)*, 2023.
- [17] Jinsung Yoon, Lydia N Drumright, and Mihaela Van Der Schaar. Anonymization through data synthesis using generative adversarial networks (ads-gan). *IEEE journal of biomedical and health informatics*, 24(8):2378–2388, 2020.

- [18] Virginia Fernandez, Pedro Sanchez, Walter Hugo Lopez Pinaya, Grzegorz Jacenków, Sotirios A Tsafaris, and Jorge Cardoso. Privacy distillation: reducing re-identification risk of multimodal diffusion models. *arXiv:2306.01322*, 2023.
- [19] Ryan Webster, Julien Rabin, Loic Simon, and Frederic Jurie. On the de-duplication of laion-2b. *arXiv:2303.12733*, 2023.
- [20] Gowthami Somepalli, Vasu Singla, Micah Goldblum, Jonas Geiping, and Tom Goldstein. Understanding and mitigating copying in diffusion models. *Advances in Neural Information Processing Systems*, 36, 2023.
- [21] Gowthami Somepalli, Vasu Singla, Micah Goldblum, Jonas Geiping, and Tom Goldstein. Diffusion art or digital forgery? investigating data replication in diffusion models. In *Proceedings of the IEEE/CVF Conference on Computer Vision and Pattern Recognition*, 2023.
- [22] Yuxin Wen, Yuchen Liu, Chen Chen, and Lingjuan Lyu. Detecting, explaining, and mitigating memorization in diffusion models. In *The Twelfth International Conference on Learning Representations*, 2024.
- [23] Pierre Chambon, Christian Bluethgen, Jean-Benoit Delbrouck, Rogier Van der Sluijs, Małgorzata Połacin, Juan Manuel Zambrano Chaves, Tanishq Mathew Abraham, Shivanshu Purohit, Curtis P Langlotz, and Akshay Chaudhari. Roentgen: Vision-language foundation model for chest x-ray generation. *arXiv preprint arXiv:2211.12737*, 2022.
- [24] Edward J Hu, yelong shen, Phillip Wallis, Zeyuan Allen-Zhu, Yuanzhi Li, Shean Wang, Lu Wang, and Weizhu Chen. LoRA: Low-rank adaptation of large language models. In *ICLR*, 2022.
- [25] Dawid Jan Kopiczko, Tijmen Blankevoort, and Yuki M Asano. VeRA: Vector-based random matrix adaptation. In *The Twelfth International Conference on Learning Representations*, 2024.
- [26] Shih-Yang Liu, Chien-Yi Wang, Hongxu Yin, Pavlo Molchanov, Yu-Chiang Frank Wang, Kwang-Ting Cheng, and Min-Hung Chen. Dora: Weight-decomposed low-rank adaptation. *arXiv:2402.09353*, 2024.
- [27] Dongze Lian, Daquan Zhou, Jiashi Feng, and Xinchao Wang. Scaling & shifting your features: A new baseline for efficient model tuning. *Advances in Neural Information Processing Systems*, 35:109–123, 2022.
- [28] Ligong Han, Yinxiao Li, Han Zhang, Peyman Milanfar, Dimitris Metaxas, and Feng Yang. Svdiff: Compact parameter space for diffusion fine-tuning. *arXiv:2303.11305*, 2023.
- [29] Enze Xie, Lewei Yao, Han Shi, Zhili Liu, Daquan Zhou, Zhaoqiang Liu, Jiawei Li, and Zhenguo Li. DiffFit: Unlocking transferability of large diffusion models via simple parameter-efficient fine-tuning. *arXiv:2304.06648*, 2023.
- [30] Alistair EW Johnson, Tom J Pollard, Lu Shen, Li-wei H Lehman, Mengling Feng, Mohammad Ghassemi, Benjamin Moody, Peter Szolovits, Leo Anthony Celi, and Roger G Mark. Mimic-iii, a freely accessible critical care database. *Scientific data*, 2016.
- [31] Nicholas Carlini, Florian Tramèr, Eric Wallace, Matthew Jagielski, Ariel Herbert-Voss, Katherine Lee, Adam Roberts, Tom Brown, Dawn Song, Ulfar Erlingsson, et al. Extracting training data from large language models. In *30th USENIX Security Symposium (USENIX Security 21)*, 2021.
- [32] Muhammad Usman Akbar, Wuhao Wang, and Anders Eklund. Beware of diffusion models for synthesizing medical images—a comparison with gans in terms of memorizing brain mri and chest x-ray images. *Available at SSRN 4611613*, 2023.
- [33] Salman Ul Hassan Dar, Arman Ghanaat, Jannik Kahmann, Isabelle Ayx, Theano Papavassiliu, Stefan O Schoenberg, and Sandy Engelhardt. Investigating data memorization in 3d latent diffusion models for medical image synthesis. In *International Conference on Medical Image Computing and Computer-Assisted Intervention*, 2023.
- [34] Ali Naseh, Jaechul Roh, and Amir Houmansadr. Memory triggers: Unveiling memorization in text-to-image generative models through word-level duplication. *arXiv:2312.03692*, 2023.
- [35] Jie Ren, Yaxin Li, Shenglai Zen, Han Xu, Lingjuan Lyu, Yue Xing, and Jiliang Tang. Unveiling and mitigating memorization in text-to-image diffusion models through cross attention. *arXiv:2403.11052*, 2024.

- [36] Zhenting Wang, Chen Chen, Lingjuan Lyu, Dimitris N Metaxas, and Shiqing Ma. Diagnosis: Detecting unauthorized data usages in text-to-image diffusion models. In *The Twelfth International Conference on Learning Representations, 2023*.
- [37] Alexandre Sablayrolles, Matthijs Douze, Cordelia Schmid, and Hervé Jégou. Radioactive data: tracing through training. In *International Conference on Machine Learning*, pages 8326–8335. PMLR, 2020.
- [38] Christoph Schuhmann, Romain Beaumont, Richard Vencu, Cade Gordon, Ross Wightman, Mehdi Cherti, Theo Coombes, Aarush Katta, Clayton Mullis, Mitchell Wortsman, et al. Laion-5b: An open large-scale dataset for training next generation image-text models. *Advances in Neural Information Processing Systems*, 2022.
- [39] Raman Dutt, Dylan Mendonca, Huai Ming Phen, Samuel Broida, Marzyeh Ghassemi, Judy Gichoya, Imon Banerjee, Tim Yoon, and Hari Trivedi. Automatic localization and brand detection of cervical spine hardware on radiographs using weakly supervised machine learning. *Radiology: Artificial Intelligence*, 2022.
- [40] Hugo Touvron, Matthieu Cord, Alaeldin El-Nouby, Jakob Verbeek, and Hervé Jégou. Three things everyone should know about vision transformers. In *ECCV, 2022*.
- [41] Elad Ben Zaken, Yoav Goldberg, and Shauli Ravfogel. BitFit: Simple parameter-efficient fine-tuning for transformer-based masked language-models. In *ACL*, May 2022.
- [42] Samyadeep Basu, Daniela Massiceti, Shell Xu Hu, and Soheil Feizi. Strong baselines for parameter efficient few-shot fine-tuning. *arXiv*, 2023.
- [43] Edward J Hu, Yelong Shen, Phillip Wallis, Zeyuan Allen-Zhu, Yuanzhi Li, Shean Wang, Lu Wang, and Weizhu Chen. Lora: Low-rank adaptation of large language models. *arXiv:2106.09685*, 2021.
- [44] Shoufa Chen, Chongjian Ge, Zhan Tong, Jiangliu Wang, Yibing Song, Jue Wang, and Ping Luo. Adapformer: Adapting vision transformers for scalable visual recognition. *arXiv*, 2022.
- [45] Xiaohua Zhai, Joan Puigcerver, Alexander Kolesnikov, Pierre Ruysen, Carlos Riquelme, Mario Lucic, Josip Djolonga, Andre Susano Pinto, Maxim Neumann, Alexey Dosovitskiy, et al. A large-scale study of representation learning with the visual task adaptation benchmark. *arXiv:1910.04867*, 2019.
- [46] Raman Dutt, Linus Ericsson, Pedro Sanchez, Sotirios A Tsaftaris, and Timothy Hospedales. Parameter-efficient fine-tuning for medical image analysis: The missed opportunity. *arXiv*, 2023.
- [47] Raman Dutt, Ondrej Bohdal, Sotirios A. Tsaftaris, and Timothy Hospedales. Fairtune: Optimizing parameter efficient fine tuning for fairness in medical image analysis. In *The Twelfth International Conference on Learning Representations, 2024*.
- [48] Shruthi Bannur, Stephanie Hyland, Qianchu Liu, Fernando Perez-Garcia, Maximilian Ilse, Daniel C Castro, Benedikt Boecking, Harshita Sharma, Kenza Bouzid, Anja Thieme, et al. Learning to exploit temporal structure for biomedical vision-language processing. In *Proceedings of the IEEE/CVF Conference on Computer Vision and Pattern Recognition, 2023*.
- [49] Ching-Yuan Bai, Hsuan-Tien Lin, Colin Raffel, and Wendy Chi-wen Kan. On training sample memorization: Lessons from benchmarking generative modeling with a large-scale competition. In *Proceedings of the 27th ACM SIGKDD Conference on Knowledge Discovery & Data Mining, 2021*.
- [50] Gao Huang, Zhuang Liu, Laurens Van Der Maaten, and Kilian Q Weinberger. Densely connected convolutional networks. In *Proceedings of the IEEE conference on computer vision and pattern recognition, 2017*.
- [51] Joseph Paul Cohen, Mohammad Hashir, Rupert Brooks, and Hadrien Bertrand. On the limits of cross-domain generalization in automated x-ray prediction. In *Medical Imaging with Deep Learning, 2020*.
- [52] Robin Rombach, Andreas Blattmann, Dominik Lorenz, Patrick Esser, and Björn Ommer. High-resolution image synthesis with latent diffusion models. In *Proceedings of the IEEE/CVF Conference on Computer Vision and Pattern Recognition (CVPR)*, pages 10684–10695, June 2022.

- [53] Patrick von Platen, Suraj Patil, Anton Lozhkov, Pedro Cuenca, Nathan Lambert, Kashif Rasul, Mishig Davaadorj, Dhruv Nair, Sayak Paul, William Berman, Yiyi Xu, Steven Liu, and Thomas Wolf. Diffusers: State-of-the-art diffusion models. <https://github.com/huggingface/diffusers>, 2022.
- [54] Olaf Ronneberger, Philipp Fischer, and Thomas Brox. U-net: Convolutional networks for biomedical image segmentation. In *Medical image computing and computer-assisted intervention—MICCAI 2015: 18th international conference, Munich, Germany, October 5-9, 2015, proceedings, part III 18*. Springer, 2015.
- [55] Alec Radford, Jong Wook Kim, Chris Hallacy, Aditya Ramesh, Gabriel Goh, Sandhini Agarwal, Girish Sastry, Amanda Askell, Pamela Mishkin, Jack Clark, et al. Learning transferable visual models from natural language supervision. In *International conference on machine learning*. PMLR, 2021.
- [56] Diederik P Kingma and Max Welling. Auto-encoding variational bayes. *arXiv:1312.6114*, 2013.
- [57] Kalyanmoy Deb, Amrit Pratap, Sameer Agarwal, and TAMT Meyarivan. A fast and elitist multiobjective genetic algorithm: Nsga-ii. *IEEE transactions on evolutionary computation*, 6(2):182–197, 2002.
- [58] Takuya Akiba, Shotaro Sano, Toshihiko Yanase, Takeru Ohta, and Masanori Koyama. Optuna: A next-generation hyperparameter optimization framework. In *KDD*, 2019.
- [59] Ilya Loshchilov and Frank Hutter. Decoupled weight decay regularization. In *ICLR*, 2018.
- [60] Jeremy Howard. Imagenette: A smaller subset of 10 easily classified classes from imagenet, March 2019.
- [61] Chendong Xiang, Fan Bao, Chongxuan Li, Hang Su, and Jun Zhu. A closer look at parameter-efficient tuning in diffusion models. *arXiv:2303.18181*, 2023.
- [62] Jae-hun Shim, Kyeongbo Kong, and Suk-Ju Kang. Core-set sampling for efficient neural architecture search. *arXiv*, 2021.
- [63] Savan Visalpara, Krishnateja Killamsetty, and Rishabh Iyer. A data subset selection framework for efficient hyper-parameter tuning and automatic machine learning. In *ICML Workshops*, 2021.

A Appendix

A.1 Qualitative Examples

We present several qualitative examples in this section. In Figure 3, we illustrate the comparison in generation quality and memorization between a conventional fine-tuning method (Full FT), adopting a mitigation strategy with conventional fine-tuning (Full FT + RWA) and our method. Upon a close inspection, it can be observed that full fine-tuning leads to near-duplicates of the original image (col. 1 and 2). Using a mitigation mechanism such as RWA reduces the number of duplicates but decreases the image generation quality (col 3 and 4). Our solution, *MemControl*, preserves both image quality and prevents the generation of duplicate samples.

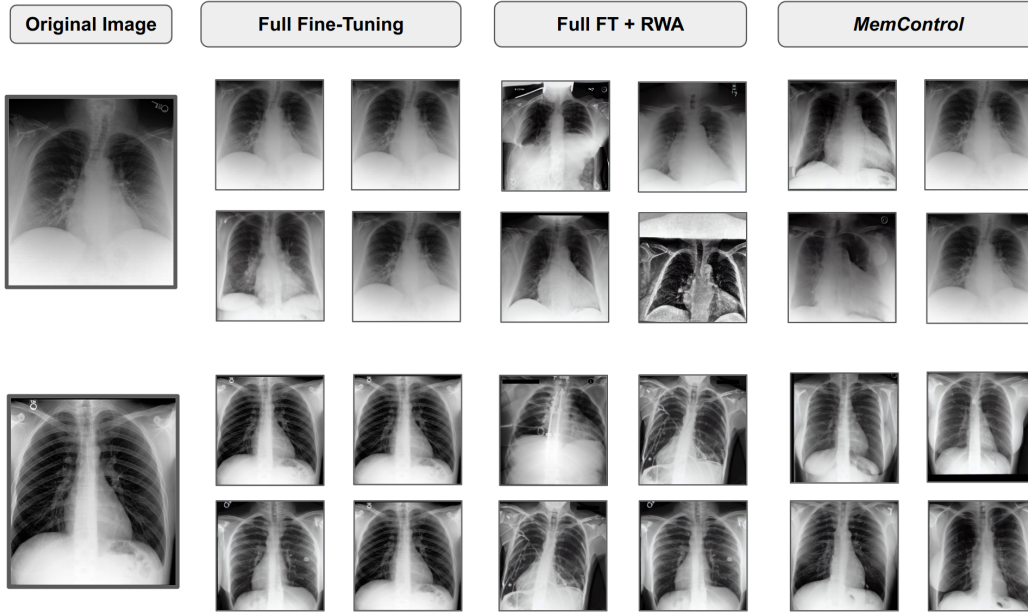


Figure 3: Plot illustrating a qualitative comparison between full fine-tuning (Full FT), Full FT + RWA, and *MemControl*. Full FT (col. 1 & 2) generates images that are near-replicas of the original training image. Combining Full FT with RWA mitigation strategy (col. 3 & 4) diversifies the generated images but deteriorates the quality. *MemControl* (col. 5 & 6) preserves image quality and prevents generating identical images.

Figure 4 illustrates some of the memorized samples obtained through the image extraction attack [16]. For each original image, multiple generations across different seeds have been shown.

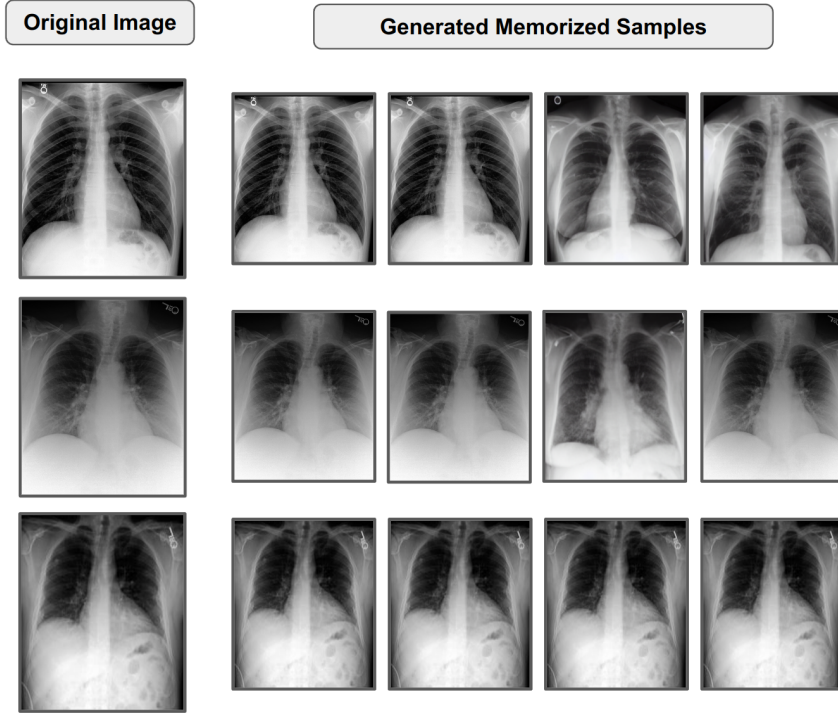


Figure 4: Plot illustrating that conventional full fine-tuning leads to the generation of memorized samples for the same prompt across multiple different seeds.

B Analysis of the Compute Cost

In this section, we analyze the compute cost of our approach and the different baselines. We use hyperparameter optimization (HPO) for each of them. Each HPO trial was conducted on 1% of the original MIMIC dataset (1100 samples) combined with 100 image-text pairs from the memorization subset, repeated 50 times (5000 samples), resulting in a total of 6100 samples. Each trial consisted of 3000 optimization steps with a batch size of 128, requiring 2 GPU hours (GPUh) per iteration on an NVIDIA V100 GPU. In total, we ran 30 trials for *MemControl*, amounting to 60 GPU hours for the entire process. We compare our approach with tuned baselines. For example, full FT required 10 similar HPO trials to determine the optimal learning rate, totalling 20 GPU hours. Table 5 summarizes the compute requirement for each experiment and baseline.

Table 5: An analysis of the compute cost in GPU hours for the different fine-tuning and memorization mitigation strategies. *Tuned Baseline* refers to the baseline obtained after searching for the optimal learning rate and other hyperparameters.

Method	Compute Cost
Full FT/ SV-DIFF/ DiffFit/ Attention (Tuned Baseline)	20 hours
Full FT/ SV-DIFF/ DiffFit/ Attention + RWA(Tuned Baseline)	27 hours
Full FT/ SV-DIFF/ DiffFit/ Attention + Threshold Mitigation (Tuned Baseline)	35 hours
<i>MemControl (ours)</i>	60 hours

C Further Discussion on Experimental Details and Results

C.1 Creating the Memorization Subset

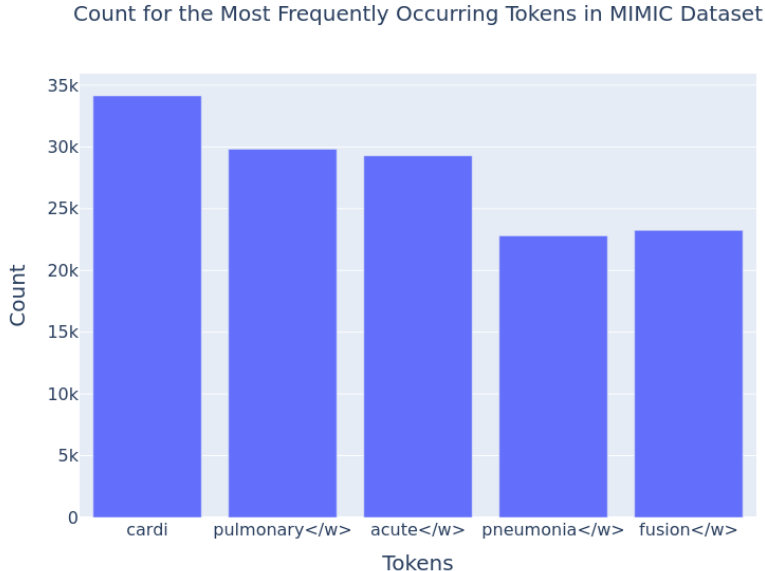


Figure 5: Count for the most frequently occurring tokens in the MIMIC dataset.

The memorization subset was created with the objective of forcing the model to memorize specific image-text pairs within the dataset during training and measuring memorization on these specific samples for reporting to the HPO. First, we identified the most frequently occurring tokens within all text captions in the MIMIC dataset (Figure 5). As a next step, we selected 100 text captions having the highest count of these particular tokens. These 100 image-text pairs constituted our *memorization subset*. During training, this subset was duplicated 50 times resulting in 5000 additional samples.

C.2 Results with Random Word Addition (RWA)

Random Word Addition (RWA) has been proposed as a successful mitigation strategy in [20]. The method involves replacing tokens/words in the caption with a random word. This method turned out to be the most successful mitigation strategy in the analysis performed in [20]. However, our results indicate that RWA often leads to a substantial decrease in generative performance. A simple explanation for this observation is that medical vocabulary, and hence prompts in a medical dataset, are very different from those in a dataset containing natural images. Since the stable diffusion pipeline uses a tokenizer trained on *natural* prompts, it often lacks significant knowledge about the specific medical terminology used in medical datasets. RWA works by generating a random integer (between 0 and 49,400) and decoding that integer into the corresponding text token using the tokenizer. With a non-medical tokenizer, the random word that is added often decreases the quality of the caption which in turn significantly impacts the textual guidance in generating new images. Although RWA did decrease memorization in certain cases in our experiments, it came at the cost of lower generation quality.

D Elucidating the Parameter Search Space

Our framework performs a hyperparameter search to identify the optimal locations for fine-tuning or model components for adding specific PEFT parameters. This process utilizes a binary mask where each element’s position corresponds to a specific component in the Stable Diffusion U-Net. The element’s value (0 or 1) indicates whether the parameter at that location should be frozen or fine-tuned. A similar investigation was conducted in [61], which found that modulating the placement of PEFT parameters around cross-attention blocks in the U-Net yields the best performance. Building on this insight, we constrain our search space to include both self-attention and cross-attention blocks in the U-Net for each PEFT method.

Stable Diffusion U-Net Design: The Stable diffusion U-Net is a modified version of the original model [54] with additional self-attention and cross-attention blocks for textual guidance. Architecturally, the model is divided into 4 *down-blocks*, 1 *mid-block*, and 4 *up-blocks*. The self-attention and cross-attention blocks are contained in the *mid-block*, more specifically in the first and the last three down and up blocks respectively.

D.1 Search Space for SV-DIFF

SV-DIFF [28] starts by conducting a Singular Value Decomposition (SVD) on the weight matrices of a pre-trained diffusion model as a one-time calculation. During fine-tuning, the original weight matrices are kept frozen, and only the *spectral shift* parameters are updated, resulting in a very small number of parameters being adjusted (0.02% of the total parameters in the U-Net). In its original setup, SV-DIFF is applied to the weight matrices of all U-Net layers (including Conv1D, Conv2D, Linear, Embedding, LayerNorm, and GroupNorm). Building on the brief investigation in [28] regarding the fine-tuning of spectral shifts within specific parameter subsets of the U-Net, we define our search space to include all self-attention and cross-attention blocks within the U-Net.

Given that there are 6 attention blocks (3 self-attention and 3 cross-attention) in both *down-blocks* and *up-blocks*, and 1 attention block in the *mid-block*, our search space for the binary mask is $\Omega \in \{0, 1\}^{13}$. For a binary mask of length 13, the first 6 elements represent the *down-blocks*, the next 6 elements denote the *up-blocks*, and the other element corresponds to the *mid-block*.

D.2 Search Space for DiffFit

DiffFit PEFT strategy [29] introduces learnable scale parameters γ into the diffusion model blocks. During fine-tuning, the majority of the model is frozen and only the bias, normalization, class-condition module and the learnable parameters γ are updated.

Similar to SV-DIFF, we explore the various positions for adding DiffFit parameters in the attention blocks of the U-Net. Given that there are 6 attention blocks (3 self-attention and 3 cross-attention) in both *down-blocks* and *up-blocks*, and 1 attention block in the *mid-block*, our search space for the binary mask is $\Omega \in \{0, 1\}^{13}$. For a binary mask of length 13, the first 6 elements represent the *down-blocks*, the next 6 elements denote the *up-blocks*, and the other element corresponds to the *mid-block*.

E Experimental Settings for Hyperparameter Optimization (HPO)

Parameter Sampler: We use the NSGA-II algorithm [57] to sample hyperparameter values. Initially, an initial population of random solutions is generated. The objective functions are then evaluated on each solution in the population. Finally, the candidate solutions are sorted according to Pareto dominance. The algorithm maintains diversity by giving preference to solutions in less crowded regions.

Bi-level Optimization Using NSGA-II: In each trial, the NSGA-II sampler selects values for the binary mask to be used for fine-tuning. After fine-tuning, we obtain a value for the objective metric associated with the sampled mask values. Over numerous trials, the sampler identifies which values better optimize the objective metric and gives these values higher preference in the sampling process. In the case of single-objective optimization, pruning techniques such as Successive Halving (SH) can be employed for early termination of unpromising trials.

Scalability to Large Datasets: Employing our framework on the MIMIC dataset consisting of 110K training samples enabled us to test the scalability of our framework to large datasets. We randomly sampled 1% (1,100 samples) from the dataset for the HPO search, and the mask obtained on this subset was finally used for fine-tuning on the entire dataset. Previously, such sampling strategies for conducting HPO search on large datasets have been shown to be effective [47, 62, 63].

E.1 Analysis of the HPO

In this section, we present an analysis of the HPO search over different PEFT search spaces.

Convergence of the HPO: Figure 6 illustrates the outer loop convergence in the bi-level optimization for the specific case of the SV-DIFF parameter search space. The plot demonstrates that the memorization metric d^{mem} successfully converges for both parameter search spaces (SV-DIFF and DiffFit) within the given number of outer loop iterations. This indicates that the HPO search ran for a sufficient number of trials to reach the optimal objective value.

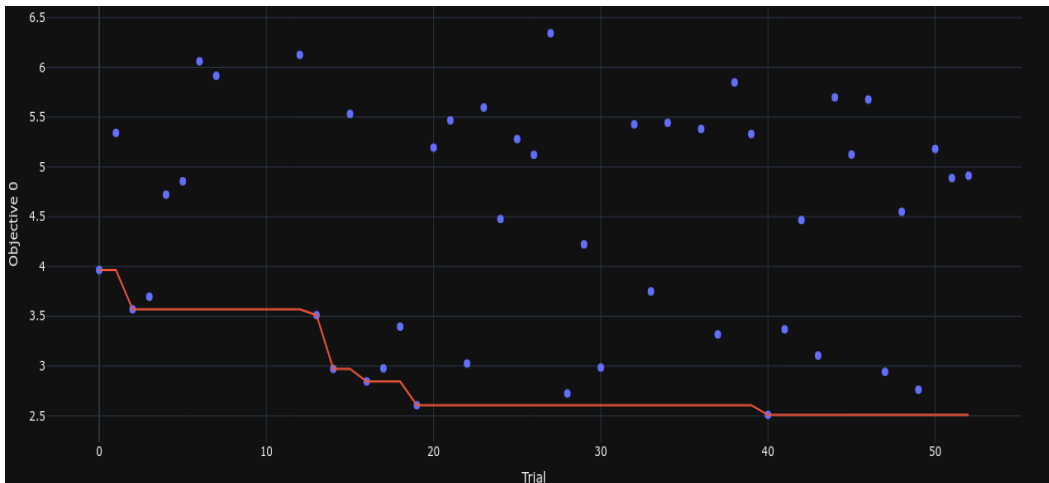


Figure 6: Figure depicting the optimization history of the memorization metric during the HPO search for SV-DIFF method.

NeurIPS Paper Checklist

1. Claims

Question: Do the main claims made in the abstract and introduction accurately reflect the paper’s contributions and scope?

Answer: [Yes]

Justification: Yes. The abstract claims to propose a bi-level optimization framework that selects optimal parameter subsets to balance both generation quality and mitigate memorization in text-to-image diffusion models. These claims have been justified and experimentally shown throughout the paper.

2. Limitations

Question: Does the paper discuss the limitations of the work performed by the authors?

Answer: [Yes]

Justification: Yes, the limitations have been discussed in Section 4.7.

3. Theory Assumptions and Proofs

Question: For each theoretical result, does the paper provide the full set of assumptions and a complete (and correct) proof?

Answer: [NA]

Justification: The paper does not contain theoretical results. However, sufficient equations have been provided at appropriate sections.

4. Experimental Result Reproducibility

Question: Does the paper fully disclose all the information needed to reproduce the main experimental results of the paper to the extent that it affects the main claims and/or conclusions of the paper (regardless of whether the code and data are provided or not)?

Answer: [Yes]

Justification: All experimental details have been provided in section 4. Additionally, the source code would be open-sourced for better reproducibility.

5. Open access to data and code

Question: Does the paper provide open access to the data and code, with sufficient instructions to faithfully reproduce the main experimental results, as described in supplemental material?

Answer: [Yes]

Justification: All the experimental details have been provided in section 4. Additionally, the source code would be open-sourced for better reproducibility.

6. Experimental Setting/Details

Question: Does the paper specify all the training and test details (e.g., data splits, hyper-parameters, how they were chosen, type of optimizer, etc.) necessary to understand the results?

Answer: [Yes]

Justification: All the experimental details have been provided in section 4. Additionally, the source code would be open-sourced for better reproducibility.

7. Experiment Statistical Significance

Question: Does the paper report error bars suitably and correctly defined or other appropriate information about the statistical significance of the experiments?

Answer: [NA]

Justification: The experiments have been run once due to computational costs, showing large improvements compared to the baselines.

8. Experiments Compute Resources

Question: For each experiment, does the paper provide sufficient information on the computer resources (type of compute workers, memory, time of execution) needed to reproduce the experiments?

Answer: [Yes]

Justification: A detailed analysis on the compute cost incurred in each experiment has been discussed and presented in Appendix B.

9. Code Of Ethics

Question: Does the research conducted in the paper conform, in every respect, with the NeurIPS Code of Ethics <https://neurips.cc/public/EthicsGuidelines>?

Answer: [Yes]

Justification: Yes, the research conducted in this work abides by the NeurIPS Code of Ethics.

10. Broader Impacts

Question: Does the paper discuss both potential positive societal impacts and negative societal impacts of the work performed?

Answer: [Yes]

Justification: The broader impacts have been discussed in Section 4.7.

11. Safeguards

Question: Does the paper describe safeguards that have been put in place for responsible release of data or models that have a high risk for misuse (e.g., pretrained language models, image generators, or scraped datasets)?

Answer: [NA]

Justification: Addition of safeguards are not applicable to the research presented in this work.

12. Licenses for existing assets

Question: Are the creators or original owners of assets (e.g., code, data, models), used in the paper, properly credited and are the license and terms of use explicitly mentioned and properly respected?

Answer: [Yes]

Justification: All the original authors and creators of the models, algorithms, and datasets used in the paper have been appropriately cited in the paper.

13. New Assets

Question: Are new assets introduced in the paper well documented and is the documentation provided alongside the assets?

Answer: [NA]

Justification: The paper does not release any new assets.

14. Crowdsourcing and Research with Human Subjects

Question: For crowdsourcing experiments and research with human subjects, does the paper include the full text of instructions given to participants and screenshots, if applicable, as well as details about compensation (if any)?

Answer: [NA]

Justification: No crowdsourcing was conducted for this work.

15. Institutional Review Board (IRB) Approvals or Equivalent for Research with Human Subjects

Question: Does the paper describe potential risks incurred by study participants, whether such risks were disclosed to the subjects, and whether Institutional Review Board (IRB) approvals (or an equivalent approval/review based on the requirements of your country or institution) were obtained?

Answer: [NA]

Justification: IRB approval was not required in this study.